



Towards model descriptions of the latest data by the NA61/SHINE collaboration on $^{40}\text{Ar} + ^{45}\text{Sc}$ and $^7\text{Be} + ^9\text{Be}$ interactions

A. Galoyan¹, A. Ribon², V. Uzhinsky^{3,a,b}

¹ V.I. Veksler and A.M. Baldin Laboratory of High Energy Physics, Joint Institute for Nuclear Research, Dubna, Moscow region 141980, Russia

² Conseil Européen pour la Recherche Nucléaire, 1211 Geneva, Switzerland

³ M.G. Meshcheryakov Laboratory of Information Technologies, Joint Institute for Nuclear Research, Dubna, Moscow region 141980, Russia

Received: 7 April 2021 / Accepted: 9 February 2022
© The Author(s) 2022

Abstract Application of the HIJING, EPOS 1.99, UrQMD and Geant4 FTF models for the analysis of experimental data by the collaboration is considered. A short description of the models is given. It is shown that the FTF (FRITIOF) model of the Geant4 toolkit describes well the NA61/SHINE data on π^- meson rapidity distributions in $^{40}\text{Ar} + ^{45}\text{Sc}$ interactions at $\sqrt{s_{NN}} = 5.2$ and 6.1 GeV. At higher energies, $\sqrt{s_{NN}} = 7.6, 8.8, 11.9$ and 16.8 GeV, the model underestimates the data by 13%, 14%, 14% and 27%, respectively. The model also describes well the analogous data for $^7\text{Be} + ^9\text{Be}$ interactions at all energies ($\sqrt{s_{NN}} = 6.1\text{--}16.8$ GeV). It is the best model description among the descriptions of other models considered by the collaboration.

Recently, the NA61/SHINE collaboration has published [1] experimental data on π^- meson production in $^{40}\text{Ar} + ^{45}\text{Sc}$ interactions at beam momenta from 13A to 150A GeV/c for 0–5% centralities. The collaboration has compared its results (rapidity distributions of π^- meson, dn/dy) with EPOS [2], UrQMD [3,4] and HIJING [5,6] model calculations. The data and the model calculations performed by the collaboration are presented in Fig. 1. As seen, the EPOS and UrQMD event generators give a satisfactory description of the data only at the momentum of 150A GeV/c. At lower energies, the EPOS model overestimates dn/dy for π^- mesons at $y \sim 0$, and the UrQMD model underestimates the data. The HIJING model overestimates the data at all energies. We also added our Geant4 FTF (Fritiof) model calculations in Fig. 1. Below we will try to understand the source of the discrepancies between the models and their nature. Thus, we give a short description of the models.

The authors are thankful to A. Seryakov, M. Naskret, S. Morozov, G.A. Feofilov, A. Ivashkin, S. Shimanskii, O. Gavrishchuk and V.I. Yurevich for useful considerations and explanations.

^a e-mail: uzhinsky@jinr.ru (corresponding author)

^b the Geant4 hadronic physics working group

The HIJING (Heavy Ion Jet Interaction Generator) model combines soft and hard interactions in the eikonal approximation [5] and uses the LUND string fragmentation algorithm (JETSET6.2) [7,8] for string hadronization and Pythia 4.8 [9] for simulations of the hard scatterings. The soft nucleon–nucleon interactions are treated on the basis of the Fritiof model [10,11]. The properties of the residual nuclei are not calculated and, correspondently, their fragmentation is not simulated. A calculation of the residual nucleus properties was proposed in [12]. The HIJING model has been widely used for more than 30 years in designing experimental setups to study nucleus–nucleus interactions at high and super high energies. Thus, checking its correctness is very important.

The EPOS 1.99 model implements the Gribov–Regge theory for the calculations of cross sections and probabilities of nucleus–nucleus interactions. Only pomeron exchanges are taken into account. Non-vacuum reggeon exchanges are not considered. Thus, there can be a problem in applying the model at low energies. The VENUS model [13] is used in the EPOS generator for simulations of string fragmentation and hard scatterings. As stated in [14] in the application of the generator to the $^7\text{Be} + ^9\text{Be}$ reactions, “The EPOS generator includes the fragment coalescence and, therefore, produces nuclear fragments. The momenta of fragments, as well as spectator protons and neutrons, were smeared with the Fermi motion momentum”. The model is very popular in cosmic ray studies.

The UrQMD (the Ultra-relativistic Quantum Molecular Dynamics) model [3,4] uses the Glauber approximation taking into account the particle formation time for calculations of the interaction probabilities. The simulation of particle production is done in the framework of the Fritiof model, enlarged by quark exchange processes, which allows to extend it to low energies. From our point of view, this extension is unsuccessful because the pion production in pp interactions at $P_{lab} = 20\text{--}80$ GeV/c is underestimated [15,16].

Nuclear residuals are not considered in the UrQMD generator. Only spectator off-shell nucleons are written in the model output file, of course, with produced mesons and on-shell baryons. Residual accounting was proposed in [17].

The Geant4 FTF generator is an implementation of the Fritiof model in the Geant4 framework. The Geant4 package [18] is a toolkit for the simulation of the particle propagation in matter. It also allows to estimate the detector response. Thus, it is used by many experimental groups all over the world, and especially by all LHC collaborations for design, calibration and study of their detectors. Since the range of particle energies varies from low energy radioactive decay to cosmic ray energies and LHC energies, Geant4 collects all available knowledge on the particle interaction with the nuclei, and the appropriate simulation codes and methods.

Two models are implemented in Geant4 for the simulation of hadronic interactions at high energies – the quark–gluon string (QGS) model [19–21] and the Fritiof (FTF) model [10, 11]. The QGS model is described in [22]. A short description of the FTF model is presented below, but more details are available in the Geant4 Physics Reference Manual [23].

The Fritiof model/generator [11] has been widely applied for the simulations of hadron–nucleon, hadron–nucleus and nucleus–nucleus interactions. The model assumes that all nucleon–nucleon interactions are binary reactions with the creation of resonances and excited nucleons in the final states. The spectrum of squared masses of excited nucleons is a key element of the model. We decided to parameterize the spectrum as $a/M_x^2 + b$. $a = c/\ln(M_{x,\max}^2/M_{x,\min}^2)$, $b = (1 - c)/(M_{x,\max}^2 - M_{x,\min}^2)$, where $M_{x,\min}^2$ and $M_{x,\max}^2$ are minimal and maximal values allowed by the kinematics of the reactions. $c = 0.55$ for non-diffractive interactions. $c = 1$ for one-vertex diffraction dissociation processes. In actual calculations, the light-cone minus variable ($P^- = E - P_z$) is used instead of M_x^2 . The excited nucleons are considered as quark–gluon strings, fragmentation of which produces hadrons. The fragmentation of strings is simulated using a modified version of the LUND algorithm [7, 24] implemented in the Geant4 toolkit.

The Geant4 FTF model considers the diffraction dissociation into high mass states, quark-exchange processes and non-diffractive interactions. The phenomenological parametrizations of the corresponding cross sections are implemented in Geant4 (see details in the Geant4 Physics Reference Manual [23]). For simulations of nucleus–nucleus interactions, we apply a simplified Glauber approximation. The Fermi motion of nuclear nucleons is taken into account according to the method of Refs. [12, 25]. Fine tuning of the FTF model parameters has been done using the NA61/SHINE data on pp interactions at various energies [26].

The Glauber approach underestimates the multiplicity of the fast ejected target nucleons in hadron–nucleus interactions. It is necessary to add the cascading of secondary particles in the nuclei. We simulate the cascading in the FTF generator within the Reggeon Theory Inspired Model (RTIM) [27–29]. The excitation energies of the residual nuclei are estimated in the wounded nucleon approximation [30]. The excited residuals evaporate nucleons and produce nuclear fragments. Thus, the FTF model is the only one of the models considered which takes into account nuclear fragment creation.

Particles and nuclear fragments generated by the FTF model were passed through the residual magnetic field of the NA61/SHINE setup. The process was not simulated directly, instead we used so-called “acceptance maps” as it was proposed by the collaboration [1]. The maps allow one to determine which particles will reach the Projectile Spectator Detector (PSD), and which of them will be detected by selected modules of PSD at a given beam energy. A configuration of the modules depends on the energy. The maps are parts of C++ or ROOT codes for all considered energies [31]. The code gives “Yes” or “No” for each particle or nuclear fragment.

PSD measured the energy carried by the “projectile spectators” (E_{PSD}). We determined a forward energy (E_F) of particles reaching sensitive parts of PSD as a sum of energies of mesons and gammas, and kinetic energies of baryons and nuclear fragments. E_{PSD} is affected by energy resolution, leakage of energy through rear side of PSD, saturation of photo-diodes’ current and so on. Thus, distributions of E_{PSD} and E_F are very different, though there was a correspondence between low energy parts of the distributions only for FTF events.

“For data analysis the event selection was based on ~ 5% of collisions with the lowest value of the energy E_{PSD} measured by a subset of PSD modules” (for $^{40}\text{Ar} + ^{45}\text{Sc}$ interactions) [1]. The same was done for selections of 20% of the central events in $^7\text{Be} + ^9\text{Be}$ collisions. We reproduced the selections using calculated E_F .

The Geant4 FTF model result for the rapidity distributions of π^- mesons in $^{40}\text{Ar} + ^{45}\text{Sc}$ interactions are presented in Fig. 1 together with the experimental data for 0–5% centralities. We used for the event selection the acceptance maps. In our previous publication [32] we did not do this. As seen in Fig. 1, we describe quite well the rapidity distributions of π^- mesons at beam momenta of 13A and 19A GeV/c. At higher momenta, we underestimate the data.¹

The HIJING and EPOS model results can be obtained using the Cosmic Ray Monte Carlo (CRMC) package, which is freely available [33]. The collaboration used CRMC ver-

¹ In the calculations we used Geant4 version 10.7 with minimal changes that will be included in the next release.

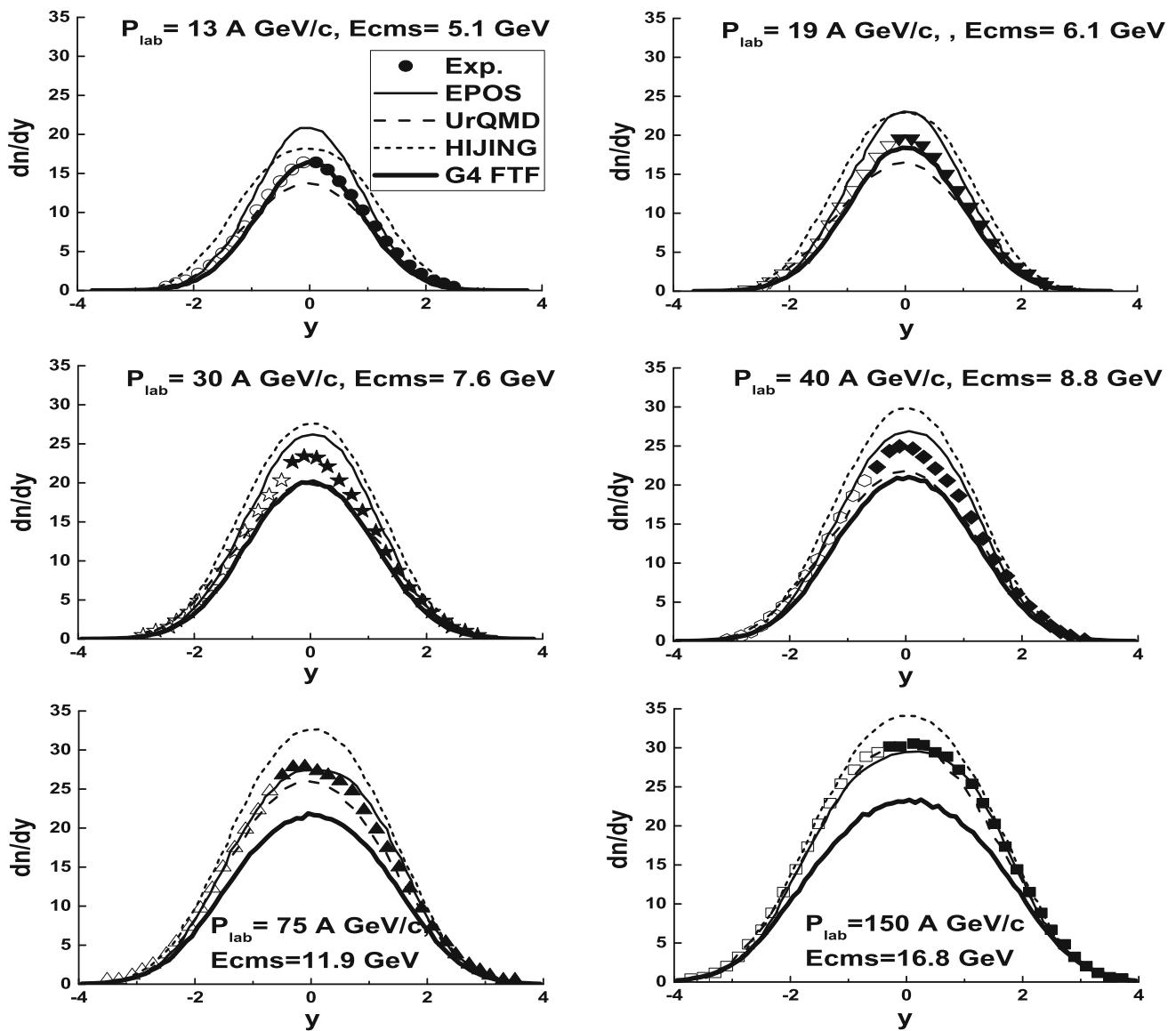


Fig. 1 Rapidity distributions, dn/dy , of π^- mesons for six beam momenta in $^{40}\text{Ar} + ^{45}\text{Sc}$ interactions. The black points are the data measured by the NA61/SHINE collaboration for 0–5% centralities. The open points are the values extrapolated by the collaboration into an unmeasured region. All experimental uncertainties are smaller than the

symbol size. The predictions of the EPOS, UrQMD and HIJING models obtained by the collaboration [1] are shown by thin solid, long and short dashed lines, respectively. The FTF model results are shown by thick solid lines

sion 1.5.3 for the EPOS model. We could not install this version. Thus, we used version 1.8.0.

CRMC writes to the output file for EPOS calculations the identifiers and kinematical properties of the produced particles – gammas, mesons, participating nucleons, Λ -hyperons and, sometimes, light nuclear fragments and one or two heavy fragments of projectile or target remnants. The spectator nucleons and nuclear fragments are missing in the analogous file for the HIJING model. Thus, the acceptance maps can be applied for EPOS calculations, and cannot be used for HIJING events.

It is obvious that the multiplicity of the mesons produced should be maximal for pure central interactions with the impact parameter $b = 0$. The corresponding events can be generated by CRMC putting “set bminim 0” and “set bmaxim 0” to the input file of the CRMC parameters ($bin/crmc.param$). The calculated distributions of π^- mesons in this case are shown in Fig. 2 for the HIJING model by the long dashed lines. As seen, our calculations are regularly below the NA61/SHINE calculations. This leads us to believe that the collaboration results are not correct.

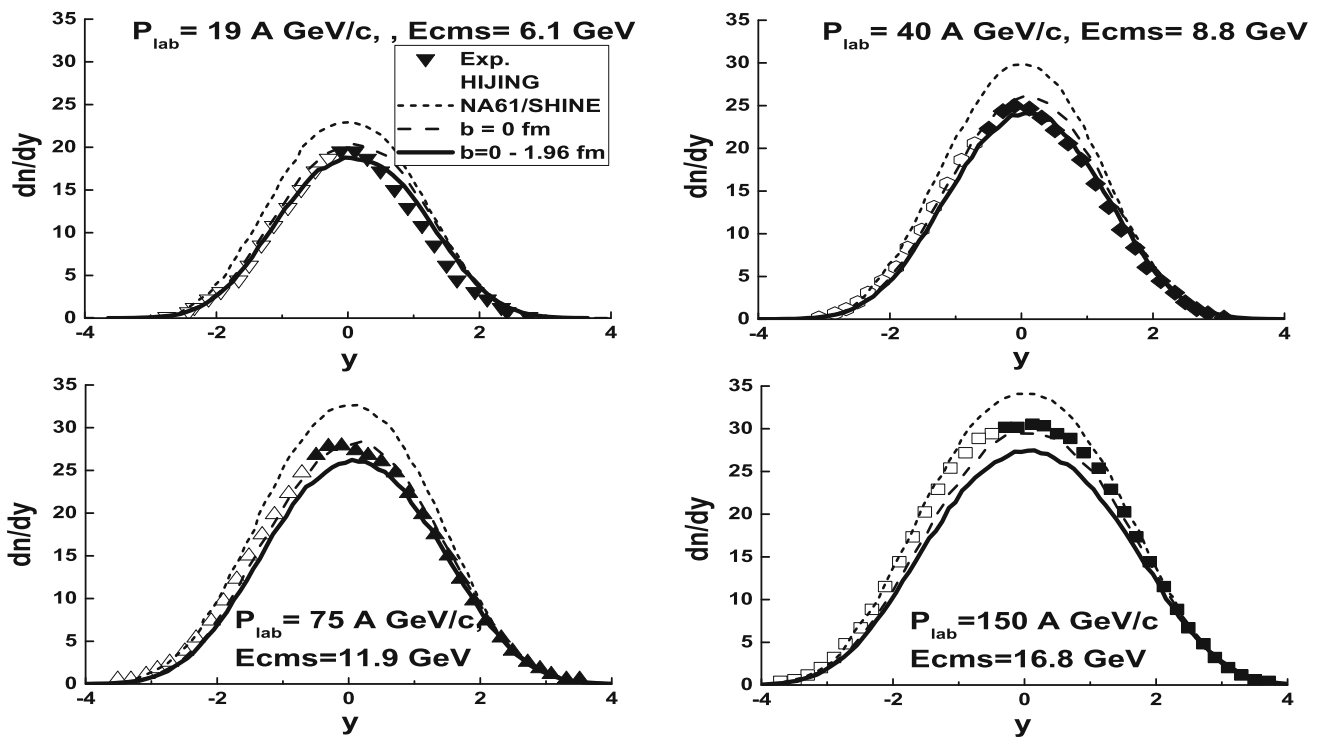


Fig. 2 Rapidity distributions, dn/dy , of π^- mesons in $^{40}\text{Ar} + ^{45}\text{Sc}$ interactions. The black points are the data measured by the NA61/SHINE collaboration for 0–5% centralities. The open points are the values extrapolated by the collaboration into an unmeasured region.

The simplest way to simulate central events is to sample the impact parameter in the interval $[0 - b_{\text{max}}]$ with a quadratic measure, where b_{max} is determined from the relation $\pi b_{\text{max}}^2 = c \sigma_{AB}^{\text{in}}$. c in our case is equal to 0.05. σ_{AB}^{in} is the inelastic cross section of the $^{40}\text{Ar} + ^{45}\text{Sc}$ interactions. According to Geant4, $\sigma_{AB}^{\text{in}} \simeq 2432$ mb, and $b_{\text{max}} \simeq 1.96$ fm. By entering the appropriate command in `bin/crmc.param` – “set bminim 0” and “set bmaxim 1.96”, we have typical HIJING model results presented in Fig. 2 by solid lines. First of all, HIJING well reproduces dn/dy of π^- mesons at $P_{\text{lab}} = 13, 19, 30$ and 40 A GeV/c. Only results at 19 and 40 A GeV/c are shown in Fig. 2. At larger energies (75 and 150 A GeV/c), the model underestimates the data.

In order to check the procedure, we did the same for EPOS model calculations, and obtained results presented in Fig. 3. As seen, our results are very close to the collaboration calculations. Thus, the application of the acceptance maps is not essential for model calculations.

The most important thing is that we reproduce the tendency observed by the collaboration – the EPOS model overestimates the data at low energies and is close to the data at high energies. The difference at low energies can be explained by imperfect parameterization of the nucleon–nucleon cross sections, insufficient reduction of the

The HIJING model calculations presented by the collaboration [1] are shown by short dashed lines. The dashed lines are our results for $b = 0$. The solid lines were obtained for $b = 0-1.96$ fm

string multiplicity, or the omission of non-vacuum reggeon exchanges. These are all very complicated questions. However, a simple way to improve the agreement at low energies is to increase the interval of the impact parameter. The results for the increasing at $b_{\text{max}} = 3.1$ fm are shown in Fig. 3 by thick solid lines. It is natural that the results at high energies are lower in this case. The latest results are very close to our previous ones published in Ref. [32]. We presented there calculations performed without quark exchange processes, such as $p + p \rightarrow n + \Delta^{++}$. Thus, we consider the coincidence of the model results as an indication of the need to improve the simulation of quark exchange processes in the EPOS model.

Since there was nothing in Ref. [1] about the selection of central events for the UrQMD model, we applied our simplified method – sampling of the impact parameter in the range $[0-1.96]$ fm, and approximately reproduced the collaboration results. We also observed the above mentioned trend – the model underestimates the data at low energies, and is consistent with the data at higher energies. This is connected with the quality of the description of pp data. In Fig. 4, we show the rapidity distributions of π^- meson in pp interactions according to the UrQMD model in comparison with the NA61/SHINE experimental data [26] and other model calculations. As seen, the EPOS model describes the

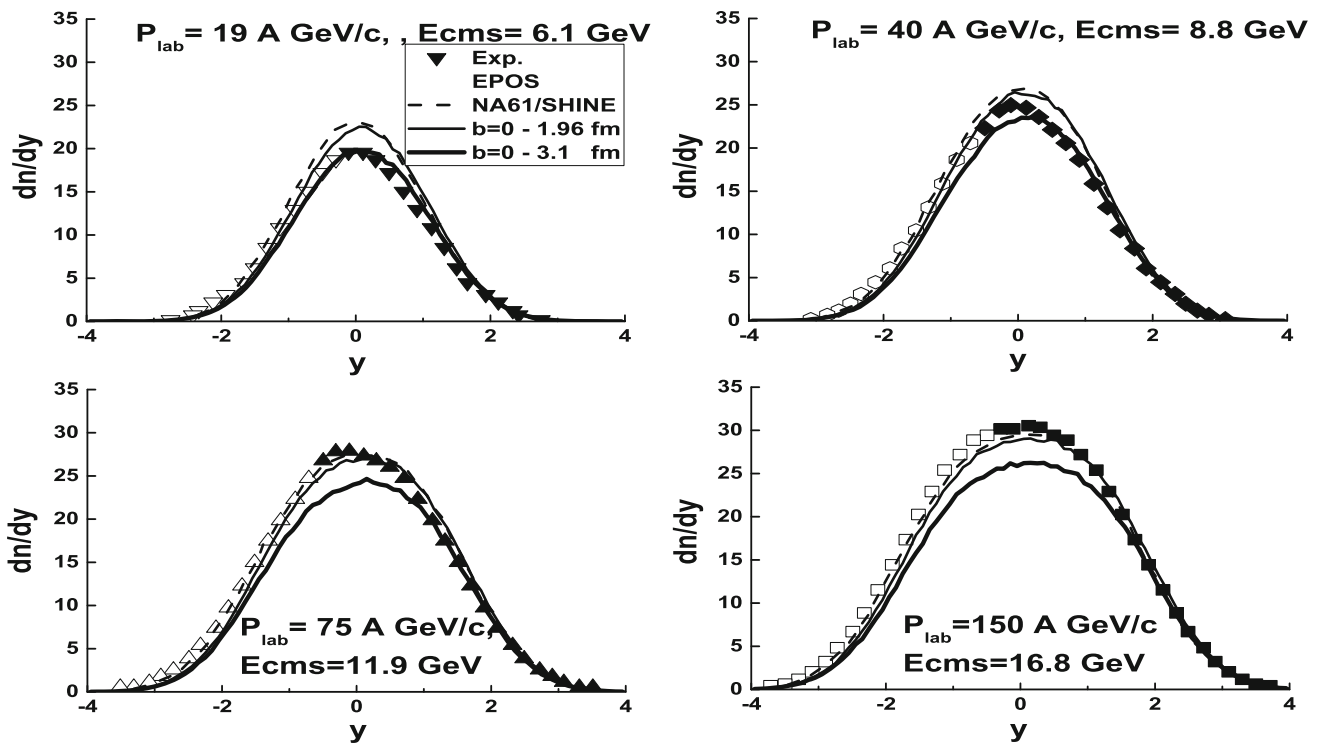


Fig. 3 Rapidity distributions, dn/dy , of π^- mesons. The black points are the data measured by the NA61/SHINE collaboration for 0–5% centralities. The open points are the values extrapolated by the collaboration into an unmeasured region. The EPOS model calculations

presented by the collaboration [1] and calculated using the acceptance maps are shown by dashed lines. The thin solid lines were obtained for $b = 0$ –1.96 fm. The thick solid lines are calculations for $b_{\max} = 3.1$ fm which corresponds to the centrality of 0–12%

data very well. The UrQMD model underestimates the data at low energies. Only at $P_{\text{lab}} = 158$ GeV/c, the model is in line with the experimental data. The Geant4 FTF model describes the data well. Only at $P_{\text{lab}} = 158$ GeV/c, the calculated curve is located below the experimental points. The latter problem can be solved by fine tuning of the quark and di-quark fragmentation parameters. The work is in progress.

The Geant4 FTF model results for $^{40}\text{Ar} + ^{45}\text{Sc}$ interactions have already been presented in Fig. 1. They agree with the data at $P_{\text{lab}} \leq 30$ A GeV/c, and they underestimate the data at higher energies. To check whether this is an internal feature of the model or a peculiarity of the data, we turn to other reactions. Recently, the NA61/SHINE collaboration has published [34] experimental data on $^7\text{Be} + ^9\text{Be}$ interactions at $P_{\text{lab}} = 19, 30, 40, 75$ and 150 A GeV/c. They are shown in Fig. 5 in a comparison with the Geant4 FTF model and EPOS model calculations. All calculations were performed taking into account the acceptance maps. As seen, the FTF model well describes the data without disagreement at high energies. Thus, we believe that something changes in the physics in $^{40}\text{Ar} + ^{45}\text{Sc}$ interactions at momenta about 19–30 A GeV/c. It is most likely due to creation of the Quark–Gluon Plasma (QGP). At least, the EPOS_LHC model [35],

which imitates effects of QGP (statistical hadronization + radial flow + azimuthal asymmetry), gives better results.

The EPOS model overestimates the data at $P_{\text{lab}} = 150$ A GeV/c in $^7\text{Be} + ^9\text{Be}$ interaction as it was noted in Ref. [34]. The same was found by the collaboration for the predictions of the UrQMD 3.4, AMPT 1.26, PHSD 4.0 and SMASH 1.6 models (see references in [34]). All these models do not consider the evaporation and fragmentation of nuclear residuals, which affect the forward energy distributions used for centrality determinations.

The correspondence between the low energy parts of the E_{PSD} distributions and E_F ones for the $^7\text{Be} + ^9\text{Be}$ collisions was worse in the EPOS model compared with FTF results. To overcome this problem, we have done our simplified selection of centrality by sampling the impact parameter in the range [0–1.92] fm in the EPOS model. The results are shown in Fig. 5 by short dashed lines. As seen, it does not significantly improve the EPOS model description of the data at $P_{\text{lab}} = 150$ A GeV/c. However, this essentially improves the form of the EPOS distributions at lower energies. The FTF calculations have been performed taking into account the acceptance maps. The FTF results for dn/dy are generally better than the EPOS ones.

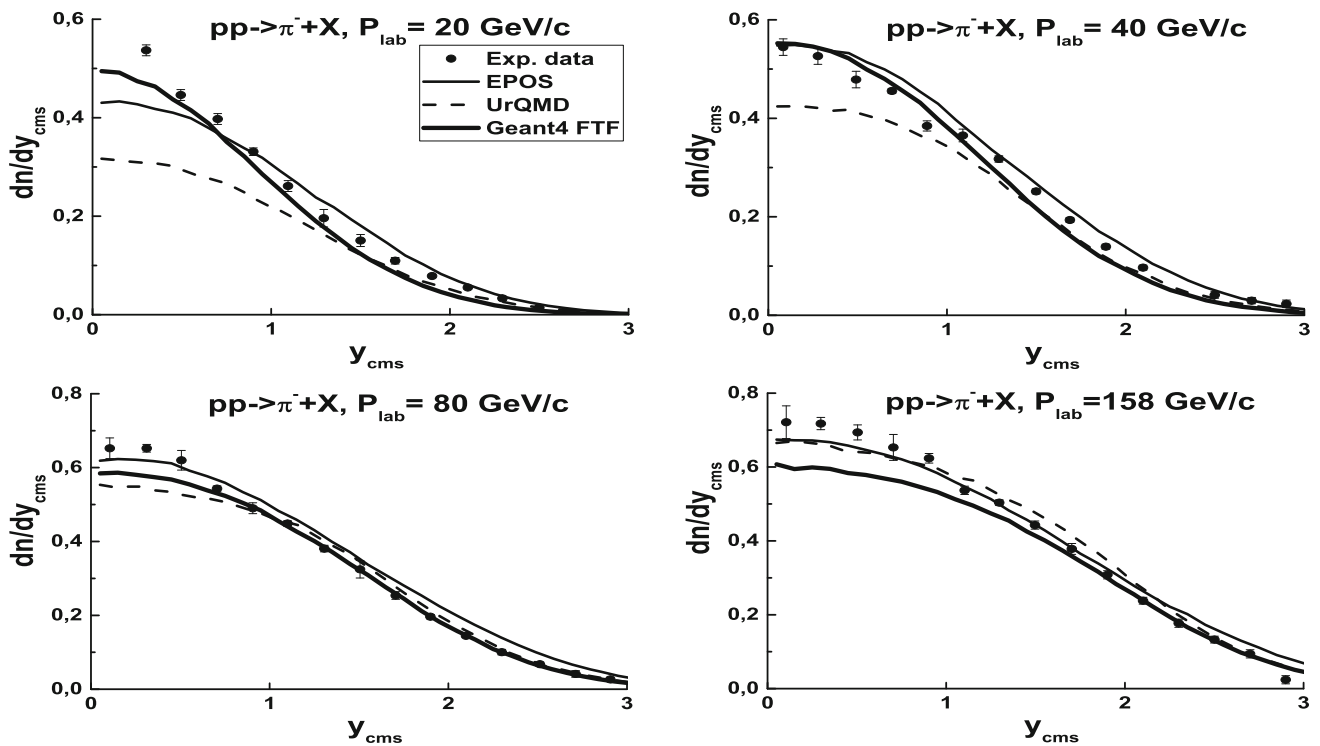


Fig. 4 Rapidity distributions, dn/dy , of π^- mesons in pp interactions. The black points are the data measured by the NA61/SHINE collaboration [26]. The EPOS model calculations are shown by thin solid lines.

The dashed lines are the UrQMD calculations. The thick solid lines are the Geant4 FTF model calculations

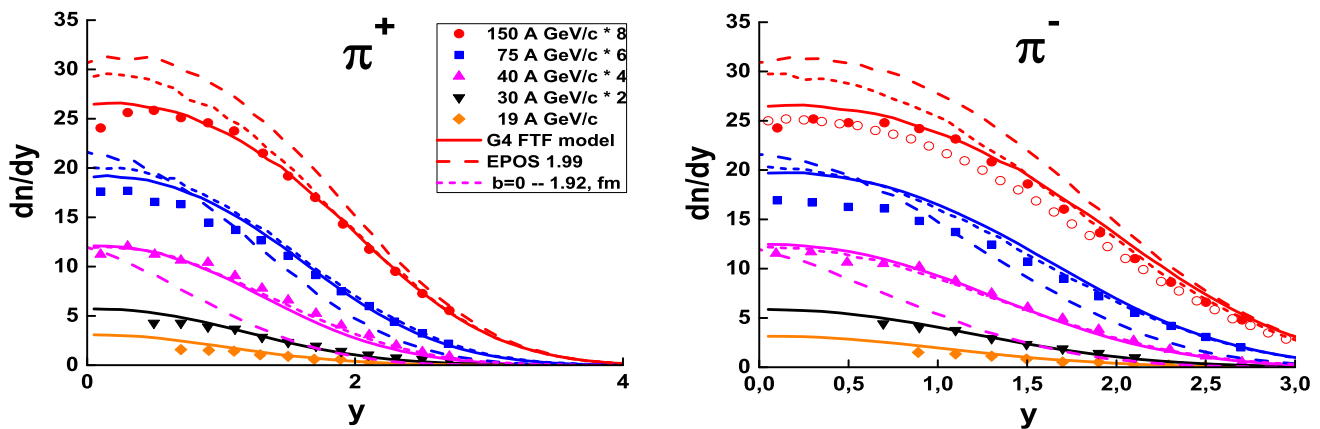


Fig. 5 Rapidity distributions of π^+ and π^- mesons in ${}^7\text{Be} + {}^9\text{Be}$ interactions. The points are the data measured by the NA61/SHINE collaboration [34]. The Geant4 FTF model calculations are shown by

solid lines. The EPOS model predictions are shown by dashed lines. The short dashed lines are the EPOS calculations for $b = 0 - 1.92$ fm

Conclusion

1. The Geant4 FTF model calculations are in good agreement with the experimental data of the NA61/SHINE collaboration on the rapidity distributions of π^- mesons produced in ${}^{40}\text{Ar} + {}^{45}\text{Sc}$ interactions at $\sqrt{s_{NN}} \leq 8$ GeV.
2. At higher energies the FTF model underestimates the dn/dy distributions of π^- mesons. These discrepancies can be compensated by incorporating the hard processes and the creation of QGP in the Geant4 FTF model.
3. The FTF model gives the best predictions for π^+ and π^- meson rapidity spectra in ${}^7\text{Be} + {}^9\text{Be}$ interactions among

other models' predictions considered by the collaboration.

4. The EPOS model should be applied with some caution due to the problem with the selection of central interactions in the generated events.
5. The latest NA61/SHINE collaboration data are very useful for checking and tuning Monte Carlo models. They can also improve our understanding of high energy–nucleus interactions.

Data Availability Statement This manuscript has no associated data or the data will not be deposited. [Authors' comment: Presented calculations can be easily reproduced. Thus, there is no need to deposit them as data.]

Open Access This article is licensed under a Creative Commons Attribution 4.0 International License, which permits use, sharing, adaptation, distribution and reproduction in any medium or format, as long as you give appropriate credit to the original author(s) and the source, provide a link to the Creative Commons licence, and indicate if changes were made. The images or other third party material in this article are included in the article's Creative Commons licence, unless indicated otherwise in a credit line to the material. If material is not included in the article's Creative Commons licence and your intended use is not permitted by statutory regulation or exceeds the permitted use, you will need to obtain permission directly from the copyright holder. To view a copy of this licence, visit <http://creativecommons.org/licenses/by/4.0/>. Funded by SCOAP³.

References

1. A. Acharya et al., [NA61/SHINE Collab.], Spectra and mean multiplicities of π^- in central $^{40}\text{Ar} + ^{45}\text{Sc}$ collisions at 13A, 19A, 30A, 40A, 75A and 150A GeV/c beam momenta measured by the NA61/SHINE spectrometer at the CERN SPS. *Eur. Phys. J. C* **81**, 397 (2021). <https://doi.org/10.1140/epjc/s10052-021-09135-3>
2. K. Werner, F.-M. Liu, T. Pierog, Parton ladder splitting and the rapidity dependence of transverse momentum spectra in deuterium–gold collisions at RHIC. *Phys. Rev. C* **74**, 044902 (2006). <https://doi.org/10.1103/PhysRevC.74.044902>
3. S.A. Bass et al., Microscopic models for ultrarelativistic heavy ion collisions. *Prog. Part. Nucl. Phys.* **41**, 255 (1998). [https://doi.org/10.1016/S0146-6410\(98\)00058-1](https://doi.org/10.1016/S0146-6410(98)00058-1)
4. M. Bleicher et al., Relativistic hadron hadron collisions in the ultrarelativistic quantum molecular dynamics model. *J. Phys. G* **25**, 1859 (1999). <https://doi.org/10.1088/0954-3899/25/9/308>
5. X.N. Wang, M. Gyulassy, HIJING: a Monte Carlo model for multiple jet production in pp, pA and AA collisions. *Phys. Rev. D* **44**, 3501 (1991). <https://doi.org/10.1103/PhysRevD.44.3501>
6. M. Gyulassy, X.N. Wang, HIJING 1.0: a Monte Carlo program for parton and particle production in high-energy hadronic and nuclear collisions. *Comput. Phys. Commun.* **83**, 307 (1994). [https://doi.org/10.1016/0010-4655\(94\)90057-4](https://doi.org/10.1016/0010-4655(94)90057-4)
7. T. Sjostrand, The Lund Monte Carlo for jet fragmentation and e+ e- Physics: Jetset Version 6.2. *Comput. Phys. Commun.* **39**, 347 (1987). [https://doi.org/10.1016/0010-4655\(86\)90096-2](https://doi.org/10.1016/0010-4655(86)90096-2)
8. T. Sjostrand, M. Bengtsson, The Lund Monte Carlo for jet fragmentation and e+ e- Physics. Jetset Version 6.3: an update. *Comput. Phys. Commun.* **43**, 347 (1987). [https://doi.org/10.1016/0010-4655\(87\)90054-3](https://doi.org/10.1016/0010-4655(87)90054-3)
9. H.-U. Bengtsson, T. Sjostrand, The Lund Monte Carlo for hadronic processes: Pythia Version 4.8. *Comput. Phys. Commun.* **46**, 43 (1987). [https://doi.org/10.1016/0010-4655\(87\)90036-1](https://doi.org/10.1016/0010-4655(87)90036-1)
10. B. Andersson, G. Gustafson, B. Nilsson-Almqvist, A model for low p_t hadronic reactions with generalizations to hadron–nucleus and nucleus–nucleus collisions. *Nucl. Phys. B* **281**, 289 (1987). [https://doi.org/10.1016/0550-3213\(87\)90257-4](https://doi.org/10.1016/0550-3213(87)90257-4)
11. B. Nilsson-Almqvist, E. Stenlund, Interactions between hadrons and nuclei: the Lund Monte Carlo, Fritiof Version 1.6. *Comput. Phys. Commun.* **43**, 387 (1987). [https://doi.org/10.1016/0010-4655\(87\)90056-7](https://doi.org/10.1016/0010-4655(87)90056-7)
12. K. Abdel-Waged, N. Felemban, Interpretation of charged-particle spectra in p + p and p + Pb collisions at energies available at the CERN Large Hadron Collider using an improved HIJING code with a collective cascade. *Phys. Rev. C* **91**, 034908 (2015). <https://doi.org/10.1103/PhysRevC.91.034908>
13. H.J. Drescher, M. Hladik, S. Ostapchenko, T. Pierog, K. Werner, Parton based Gribov–Regge theory. *Phys. Rep.* **350**, 93 (2001). [https://doi.org/10.1016/S0370-1573\(00\)00122-8](https://doi.org/10.1016/S0370-1573(00)00122-8)
14. E. Kaptur [NA61/SHINE Collab.], Analysis of collision centrality and negative pion spectra in $^7\text{Be} + ^9\text{Be}$ interactions at CERN SPS energy range. Ph.D thesis (2017). <https://edms.cern.ch/document/2004086/1>
15. V. Uzhinsky, Toward UrQMD model description of pp and pC interactions at high energies (2013). [arXiv:1308.0736](https://arxiv.org/abs/1308.0736) [hep-ph]
16. V. Uzhinsky, Toward description of pp and pC interactions at high energies: problems of Fritiof-based models (2014). [arXiv:1404.2026](https://arxiv.org/abs/1404.2026) [hep-ph]
17. K. Abdel-Waged, Improvements of ultra-relativistic quantum molecular dynamics model simulated by spallation neutron data induced by 1.2 GeV protons on Al, Fe and Zr. *J. Phys. G* **31**, 739 (2005)
18. J. Allison et al., Recent developments in Geant4. *Nucl. Instrum. Methods A* **835**, 186 (2016). <https://doi.org/10.1016/j.nima.2016.06.125>
19. A. Capella, U. Sukhatme, C.I. Tan, J. Tran Thanh Van, Dual parton model. *Phys. Rep.* **236**, 225 (1994). [https://doi.org/10.1016/0370-1573\(94\)90064-7](https://doi.org/10.1016/0370-1573(94)90064-7)
20. A.B. Kaidalov, The quark–gluon structure of the pomeron and the rise of inclusive spectra at high-energies. *Phys. Lett. B* **116**, 459 (1982). [https://doi.org/10.1016/0370-2693\(82\)90168-X](https://doi.org/10.1016/0370-2693(82)90168-X)
21. A.B. Kaidalov, K.A. Ter-Martirosian, Pomeron as quark–gluon strings and multiple hadron production at SPS collider energies. *Phys. Lett. B* **117**, 247 (1982). [https://doi.org/10.1016/0370-2693\(82\)90556-1](https://doi.org/10.1016/0370-2693(82)90556-1)
22. S. Agostinelli et al. [Geant4 collaboration], GEANT4: a simulation toolkit. *Nucl. Instrum. Methods A* **506**, 250 (2003). [https://doi.org/10.1016/S0168-9002\(03\)01368-8](https://doi.org/10.1016/S0168-9002(03)01368-8)
23. Geant4 Collaboration, Geant4 Physics Reference Manual. <http://geant4.web.cern.ch/geant4/UserDocumentation/UsersGuides/PhysicsReferenceManual/fo/PhysicsReferenceManual.pdf>
24. B. Andersson, G. Gustafson, G. Ingelman, T. Sjostrand, Parton fragmentation and string dynamics. *Phys. Rep.* **97**, 31 (1983). [https://doi.org/10.1016/0370-1573\(83\)90080-7](https://doi.org/10.1016/0370-1573(83)90080-7)
25. M.I. Adamovich et al., Complex analysis of gold interactions with photoemulsion nuclei at 10.7 GeV/nucleon within the framework of cascade and FRITIOF models. *Z. Phys. A* **385**, 331 (1997). <https://doi.org/10.1007/s002180050337>
26. A. Aduszkiewicz et al., Measurements of π^\pm , K^\pm , p and \bar{p} spectra in proton–proton interactions at 20, 31, 40, 80 and 158 GeV/c with the NA61/SHINE spectrometer at the CERN SPS. *Eur. Phys. J. C* **77**, 671 (2017). <https://doi.org/10.1140/epjc/s10052-017-5260-4>

27. K. Abdel-Waged, V.V. Uzhinsky, Model of nuclear disintegration in high-energy nucleus–nucleus interactions. *Phys. Atom. Nucl.* **60**, 828 (1997) (*Yad. Fiz.* **60** 925 (1997))
28. K. Abdel-Waged, V.V. Uzhinsky, Estimation of nuclear destruction using ALADIN experimental data. *J. Phys. G* **24**, 1723 (1997). <https://doi.org/10.1088/0954-3899/24/9/006>
29. K. Abdel-Waged, N. Felemban, V.V. Uzhinskii, GEANT4 hadronic cascade models analysis of proton and charged pion transverse momentum spectra from p + Cu and Pb collisions at 3, 8, and 15 GeV/c. *Phys. Rev. C* **84**, 014905 (2011). <https://doi.org/10.1103/PhysRevC.84.014905>
30. A.Y. Abul-Magd, W.A. Friedman, J. Hufner, Calculation of mass yields for proton nucleus spallation reactions. *Phys. Rev. C* **34**, 113 (1986). <https://doi.org/10.1103/PhysRevC.34.113>
31. A. Seryakov [NA61/SHINE Collab.], PSD acceptance maps for event selection. CERN EDMS (2017). <https://edms.cern.ch/document/1867336/1>
32. A. Galoyan, A. Ribon, V. Uzhinsky, Geant4 FTF model description of the latest data by the NA61/SHINE collaboration on $^{40}\text{Ar} + ^{45}\text{Sc}$ interactions (2021). [arXiv:2104.00937](https://arxiv.org/abs/2104.00937) [hep-ph]
33. <https://web.ikp.kit.edu/rulrich/crmc.html>
34. NA61/SHINE Collaboration (A. Acharya et al.), Measurements of π^\pm , K^\pm , pp and \bar{p} spectra in $^7\text{Be} + ^9\text{Be}$ collisions at beam momenta from 19A to 150A GeV/c with the NA61/SHINE spectrometer at the CERN SPS. *Eur. Phys. J. C* **81**, 73 (2021). https://doi.org/10.1007/978-3-030-53448-6_5
35. T. Pierog, I. Karpenko et al., EPOS LHC: test of collective hadronization with data measured at the CERN Large Hadron Collider. *Phys. Rev. C* **92**, 034906 (2015). <https://doi.org/10.1103/PhysRevC.92.034906>. [arXiv:1306.0121](https://arxiv.org/abs/1306.0121) [hep-ph]